Kinetically Controlled Photoinduced Electron Transfer Switching in Cu(I)-Responsive Fluorescent Probes

Aneese F. Chaudhry, Manjusha Verma, M. Thomas Morgan, Maged M. Henary, Nisan Siegel, Joel M. Hales, Joseph W. Perry*, Christoph J. Fahrni*

Supporting Information

Table of Contents

1. Synthetic Procedures

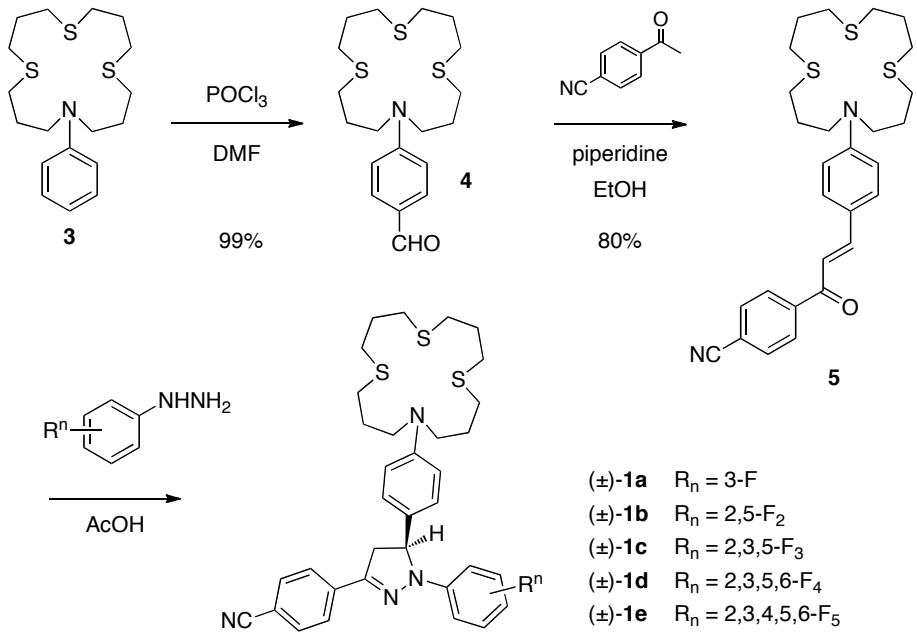

Materials and Reagents. 4-Cyanoacetophenone, 2,5-difluorophenylhydrazine (Aldrich), 3-fluorophenylhydrazine hydrochloride, 2,3,5,6-tetrafluorophenylhydrazine, pentafluorophenyl-hydrazine (Oakwood Products, West Columbia, SC); 2,3,5-trifluorophenylhydrazine, was synthesized from 1,2,3,5-tetrafluorobenzene (Aldrich) following a published procedure.[S1] NMR: δ in ppm vs $SiMe_4$ (0 ppm, ^1H, 400 MHz). MS: selected peaks; m/z. Flash chromatography (FC): Merck silica gel 60 (70-230 mesh). Thin layer chromatography (TLC): 0.25 mm, Merck silica gel 60 F_{254}, visualizing at 254 nm or with 2% $KMnO_4$ solution.

Synthesis of Pyrazolines 1a-e. General method. A mixture of chalcone **5** (0.14 mmol) and the corresponding fluoro-substituted phenylhydrazine (1.5 molar eq.) in acetic acid (3 ml) was stirred at 100 °C. Upon completion of the reaction (TLC), the mixture was cooled to room temperature and neutralized by addition of saturated sodium carbonate solution. The product was extracted with ethyl acetate, and the combined organic extracts were dried ($MgSO_4$), filtered, and concentrated under reduced pressure. The crude product was purified by flash chromatography on silica using hexane and ethyl acetate as the mobile phase.

(±)-13-(4-(3-(4-Cyanophenyl)-1-(3-fluorophenyl)-4,5-dihydro-1*H*-pyrazol-5-yl)phenyl)-1,5,9-trithia-13-azacyclohexadecane (1a). Yield: 32%. ^1H NMR ($CDCl_3$, 400 MHz) δ 1.86–1.94 (m, 8H), 2.59 (t, J = 6.8 Hz, 4H), 2.65-2.69 (m, 8H), 3.11 (dd, J = 17.1, 6.5 Hz, 1H), 3.43 (t, J = 7.1 Hz, 4H), 3.77 (dd, J = 17.1, 12.3 Hz, 1H), 5.25 (dd, J = 12.5, 6.5 Hz, 1H), 6.49 (ddt, J = 8.3, 2.4, 0.7 Hz, 1H), 6.60 (d, J = 8.8 Hz, 2H), 6.79 (ddd, J = 8.3, 2.0, 0.7 Hz, 1H), 6.89 (td, J = 11.6, 2.3 Hz, 1H), 7.06-7.13 (m, 3H), 7.64 (d, J = 11.7 Hz, 2H), 7.7 (d, J = 11.6 Hz, 2H). MS (70 eV) 618 (M^+, 100), 484 (27), 383 (22), 264 (18), 109 (15). EI HRMS *m/z* calcd for $[M]^+$ $C_{34}H_{39}FN_4S_3$ 618.2321, found 618.2314.

(±)-13-(4-(3-(4-Cyanophenyl)-1-(2,5-difluorophenyl)-4,5-dihydro-1*H*-pyrazol-5-yl)phenyl)-1,5,9-trithia-13-azacyclohexadecane (1b). Yield: 22%. ^{1}H NMR ($CDCl_3$, 400 MHz) 1.80-1.89 (m, 8H), 2.55 (t, *J* = 6.8 Hz, 4H), 2.65 (dt, *J* = 6.9, 1.6 Hz, 8H), 3.24 (dd, *J* = 16.9, 3.9 Hz, 1H), 3.37 (t, *J* = 7.1 Hz, 4H), 3.71 (dd, *J* = 16.9, 11.8 Hz, 1H), 5.65 (td, *J* = 11.7, 3.7 Hz, 1H), 6.47-6.65 (m, 3H), 6.77-6.83 (m, 1H), 6.96 (d, *J* = 8.9 Hz, 2H), 7.28-7.33 (m, 1H), 7.66 (d, *J* = 8.5 Hz, 2H), 7.86 (d, *J* = 8.4 Hz, 2H). MS (70 eV) 636 (M^+, 100), 502 (32), 401 (22), 282 (16), 127 (14). EI HRMS *m/z* calcd for $[M]^+$ $C_{34}H_{38}F_2N_4S_3$ 636.2227, found 636.2219.

(±)-13-(4-(3-(4-Cyanophenyl)-1-(2,3,5-trifluorophenyl)-4,5-dihydro-1*H*-pyrazol-5-yl)-phenyl)-1,5,9-trithia-13-azacyclohexadecane (1c). Yield: 14%. ^{1}H NMR ($CDCl_3$, 400 MHz) 1.86-1.94(m, 8H), 2.56 (t, *J* = 6.8 Hz, 4H), 2.66 (dt, *J* = 6.8, 2.6 Hz, 8H), 3.25 (dd, *J* = 16.9, 3.8 Hz, 1H), 3.39 (t, *J* = 7.1 Hz, 4H), 3.74 (dd, J = 16.9, 11.7 Hz, 1H), 5.65 (td, *J* = 11.7, 3.7 Hz, 1H), 6.43-6.36 (m, 1H), 6.49 (d, *J* = 8.8 Hz, 2H), 6.95 (d, *J* = 8.7 Hz, 2H), 7.13-7.18 (m, 1H), 7.67 (d, *J* = 11.5 Hz, 2H), 7.81 (d, *J* = 8.5 Hz, 2H). MS (70 eV) 654 (M^+, 100), 520 (31), 419 (25), 300 (14). EI HRMS *m/z* calcd for $[M]^+$ $C_{34}H_{37}F_3N_4S_3$ 654.2132, found 654.2124.

(±)-13-(4-(3-(4-Cyanophenyl)-1-(2,3,5,6-tetrafluorophenyl)-4,5-dihydro-1*H*-pyrazol-5-yl)phenyl)-1,5,9-trithia-13-azacyclohexadecane (1d). Yield: 18%. ^{1}H NMR ($CDCl_3$, 400 MHz) 1.85-1.93 (m, 8H), 2.55 (t, *J* = 6.8 Hz, 4H), 2.64-2.69 (m, 8H), 3.24 (dd, *J* = 16.9, 7.2 Hz, 1H), 3.39 (t, *J* = 7.2 Hz, 4H), 3.68 (dd, *J* = 16.9, 11.9 Hz, 1H), 5.49 (dd, *J* = 11.8, 7.1 Hz, 1H), 6.50 (d, *J* = 8.8 Hz, 2H), 6.65-6.74 (m, 1H), 7.06 (d, *J* = 14.4 Hz, 2H), 7.65 (d, *J* = 8.7 Hz, 2H), 7.75 (d, *J* = 8.7 Hz, 2H). MS (70 eV) 672 (M^+, 100), 538 (32), 437 (31), 318 (14). EI HRMS *m/z* calcd for $[M]^+$ $C_{34}H_{36}F_4N_4S_3$ 672.2038, found 672.2027.

(±)-13-(4-(3-(4-Cyanophenyl)-1-(perfluorophenyl)-4,5-dihydro-1*H*-pyrazol-5-yl)phenyl)-1,5,9-trithia-13-azacyclohexadecane (1e). Yield: 15%. ^{1}H NMR ($CDCl_3$, 400 MHz) 1.84-1.91 (m, 8H), 2.58 (t, *J* = 6.7 Hz, 4H), 2.63-2.67 (m, 8H), 3.26 (dd, *J* = 16.9, 8.09 Hz, 1H), 3.42 (t, *J* = 7.1 Hz, 4H), 3.67 (dd, *J* = 16.9, 11.7 Hz, 1H), 5.38 (d, *J* = 11.6, 8.1 Hz, 1H), 6.53 (d, *J* = 14.6 Hz, 2H), 7.08 (d, *J* = 8.7 Hz, 2H), 7.66 (d, *J* = 8.6 Hz, 2H), 7.76 (d, *J* = 8.5 Hz, 2H). MS (70 eV) 690 (M^+, 100), 556 (30), 455 (28). EI HRMS *m/z* calcd for $[M]^+$ $C_{34}H_{35}F_5N_4S_3$ 690.8555, found 690.1931.

(±)-3-(4-Cyanophenyl)-1-(3-fluorophenyl)-5-phenyl-4,5-dihydro-1*H*-pyrazole (2). Synthesized according to a previously published procedure.[S2]

13-Phenyl-1,5,9-trithia-13-azacyclohexadecane (3). N,N-Bis(3-iodopropyl)aniline[S3] (8.99 g, 21.0 mmol), bis(3-mercaptopropyl)sulfide[S4] (3.82 g, 21.0 mmol), and 1,1,3,3-tetramethylguanidine (5.3 mL, 2.0 eq) were each dissolved in acetonitrile, diluted to 10 mL, and placed in separate 10 mL syringes. The resulting solutions were simultaneously and continuously added via syringe pump over a period of 60 hours to a refluxing solution of 1,1,3,3-tetramethylguanidine (0.66 mL, 0.25 molar eq.) in acetonitrile (750 mL) under nitrogen. The reaction mixture was allowed to cool and concentrated under reduced pressure. The residue was stirred with toluene (150 mL) for one hour. The precipitated salt was filtered out, and the filtrate was chromatographed on silica gel (hexanes-*tert*-butyl methyl ether) to give the product as a colorless, viscous oil. Yield 2.40 g (32%). R_f 0.35 (8:1 hexanes-MTBE), 0.34 (10:1 Hexanes: EtOAc). ^{1}H NMR ($CDCl_3$, 400 MHz) δ 1.92 (p, *J* = 7.0 Hz, 4H), 1.95 (p, *J* = 7.1 Hz, 4H), 2.62 (t, *J* = 6.9 Hz, 4H), 2.68 (t, *J* = 6.9 Hz, 4H), 2.69 (t, *J* = 7.0 Hz, 4H), 3.46 (t, *J* = 7.2 Hz, 4H), 6.66-6.71 (m, 3H), 7.19-7.25 (m, 2H). ^{13}C NMR ($CDCl_3$, 100 MHz) δ27.5, 29.6, 29.8, 30.8, 31.0, 50.4, 112.5, 116.2, 129.2, 148.1. MS (70eV) 355 ([M^+], 100), 221 (18), 193 (17), 180 (27), 146 (46), 120 (29), 106 (26), 77 (11). EI HRMS *m/z* calcd for [M^+] $C_{18}H_{29}NS_3$ 355.1462, found 355.1458.

4-(1,5,9-Trithia-13-azacyclohexadecan-13-yl)benzaldehyde (4). Phosphorus oxychloride (5.0 mL, 55 mmol) was added in 0.5 mL aliquots over a period of 30 min to a stirring solution of dimethylformamide (8.5 mL, 110 mmol) cooled via ice bath. The resulting mixture was then added to a solution of macrocycle **3** (2.40 g, 6.75 mmol) in DMF (8 mL). The reaction flask was flushed with nitrogen, and the mixture was stirred at 75°C for 45 min. After cooling, the reaction mixture was poured into water (200 mL), and made strongly basic with sodium hydroxide. Dichloromethane (50 mL) was added, and the mixture was stirred for one hour. The organic layer was separated, and the aqueous layer was extracted with dichloromethane (2 x 50 mL). The combined organic layers were concentrated under reduced pressure. The residue was taken up in benzene (25 mL) and washed with water to remove residual DMF. The solution was then dried with sodium sulfate and concentrated under reduced pressure to give the product as a light-brown oil. Yield: 2.56 g (99%). R_f 0.44 (2:1 hexanes: EtOAc).^{1}H NMR ($CDCl_3$, 400 MHz) δ 1.93 (p, *J* = 6.9 Hz, 4H), 1.99 (p, *J* = 7.0 Hz, 4H), 2.64 (t, *J* = 6.6 Hz, 4H), 2.70 (t, *J* = 6.9 Hz, 4H), 2.72 (t, *J* = 7.0 Hz, 4H), 3.61 (t, *J* = 7.5 Hz, 4H), 6.68 (d, *J* = 9.0 Hz, 2H), 7.72 (d, *J* = 9.0 Hz, 2H), 9.73 (s, 1H). ^{13}C NMR ($CDCl_3$, 100 MHz) δ 26.9, 29.1, 29.4, 30.5, 30.9, 49.9, 110.8, 124.9, 132.0, 152.3, 189.8. MS (70eV) 383 ([M^+], 100), 249 (15), 208 (26), 174 (44), 134 (25), 87 (13), 41 (14). EI HRMS *m/z* calcd for [M^+] $C_{10}H_{29}NOS_3$ 383.1411, found 383.1392.

(*E*)-3-(4-(1,5,9-trithia-13-azacyclohexadecan-13-yl)phenyl)-1-(4-cyanophenyl)prop-2-en-1-one (5). A mixture of aldehyde **4** (0.40 g, 1.0 mmol), 4-acetylbenzonitrile (0.152 g, 1.05 mmol), and piperidine (0.22 mL, 2.3 mmol) in ethanol (3 mL) was heated at reflux overnight. The solution was cooled to room temperature, the bright orange product was filtered off, washed with diethyl ether and dried under reduced pressure to afford chalcone **5**. Yield: 80%. ^{1}H NMR ($CDCl_3$, 400 MHz) δ 1.99-1.87 (m, 8H), 2.63 (t, *J* = 6.6 Hz, 4H), 2.70 (q, *J* = 7.1 Hz, 8H), 3.58 (t, *J* = 7.2 Hz, 4H), 6.66 (d, *J* = 8.8 Hz, 2H), 7.23 (d, *J* = 15.5 Hz, 1H), 7.52 (d, *J* = 8.7 Hz, 2H), 7.79-7.75 (m, 3H), 8.05 (d, *J* = 8.2 Hz, 2H). ^{13}C-NMR ($CDCl_3$ 100 MHz) δ 27.2, 29.4, 29.6, 30.8, 31.1, 50.1, 111.8, 115.2, 115.7, 118.2, 122.0, 128.6, 131.0, 132.3, 142.5, 147.3, 150.3, 189.0. MS (70 eV) 510 (M^+, 100), 376 (25), 301 (32), 275 (35), 130 (14). EI HRMS *m/z* calcd for [M]$^+$ $C_{28}H_{34}N_2OS_3$ 510.1833, 510.1829.

Oxidative dimerization of ligand (3):

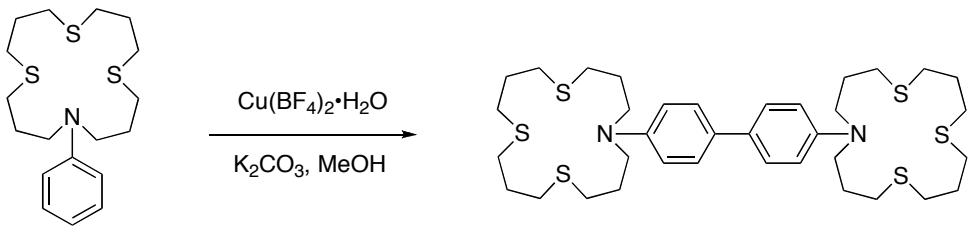

3 38% **6**

4,4'-Di(1,5,9-trithia-13-azacyclohexadecan-13-yl)biphenyl (6). Ligand **3** (156 mg, 4.40 mmol) and copper(II)tetrafluoroborate hydrate (680 mg, 5 molar eq.) were dissolved in methanol (15 mL); the resulting dark solution was shielded from light and stirred under argon for 12 h. Potassium carbonate (120 mg, 2 molar eq.) was then added, and the mixture was stirred under argon for 18 h. The mixture was then poured into 60 mL of an aqueous solution containing 0.22 M KCN, 0.07 M disodium EDTA, and 0.2 M NaOH. Dichloromethane (25 mL) was added, and the resulting blue mixture was stirred for 1 h. The organic layer was separated, and the colorless aqueous phase was extracted with an additional 25 mL of dichloromethane. The combined organic layers were washed with two 20 mL portions of the cyanide-EDTA solution, dried with sodium sulfate, concentrated under reduced pressure, and diluted with 75 mL of MTBE. The resulting solution was allowed to stand for 4 hours, then refrigerated overnight. The resulting product was collected by filtration, washed with cold MTBE, and dried under vacuum to yield 59 mg (38%) of tan solid. ^{1}H NMR ($CDCl_3$, 400 MHz) δ 1.83-2.02 (m, 16H), 2.64 (t, J = 6.8 Hz, 8H), 2.69 (t, J = 6.9 Hz, 8H) 3.47 (t, J = 7.8 Hz, 8H, broad), 6.73 (d, J = 8.9 Hz, 4H), 7.41 (d, J = 8.9 Hz, 4H). ^{13}C NMR ($CDCl_3$, 100 MHz) δ 22.3, 24.7, 34.0, 37.0, 37.76, 37.82, 65.4, 94.4, 127.1, 128.4, 128.9, 137.9. MS (70 eV) 708 ([M$^{\cdot}$], 100), 574 (8) 473 (8), 191.1 (35), 73 (15). EI HRMS *m/z* calcd for [M$^{\cdot}$] $C_{36}H_{56}N_2S_6$ 708.2768, found 708.2765.

2. Transient Absorption Data Fitting

Transient absorption data of compound **1a** acquired in pure or acidified methanol were analyzed by least squares fitting over the entire spectral range using SPECFIT.[S5] In both cases, the reaction systems were modeled based on a series of 4 non-equilibrating consecuitve first order processes using the built-in editor of SPECFIT. The data acquired in the presence of $[Cu(I)(CH_3CN)_4]PF_6$ had to be analyzed with a model composed of 3 independent species with distinct decay kinetics. Because SPECFIT does not allow for global fitting of a series of first order processes starting from multiple independent species, the transient data were analyzed only at a single wavelength using the following procedure:

Given the presence of three coordination species A, B, and C that exhibit different electron transfer kinetics, three sets of independent differential equation must be derived to describe the observed transient absorption at a single wavelength. Assuming that species A undergoes the ET reaction significantly faster than radiative deactivation, we can model the excited state dynamics of A by a series of consecutive first order reactions,

$$FC_A \xrightarrow{k_1} {}^1LE_A \xrightarrow{k_{2a}} {}^1ET_A \xrightarrow{k_3} GS_A \tag{S1}$$

where FC is the Franck-Condon state formed upon vertical excitation, ^{1}LE is the vibrationally relaxed local excited singlet state, ^{1}ET is the electron transfer (singlet) state, and GS is the ground state (with index A referring to the corresponding transient species of A).

The rate of disappearance of FC_A can be written as

$$-\frac{d[FC_A]}{dt} = k_1[FC_A] \tag{S2}$$

The net change in concentration of the successor state ^1LE_A corresponds to the rate k_1 at which it is formed, minus the rate k_{2a} at which it decays:

$$\frac{d[^1LE_A]}{dt} = k_1[FC_A] - k_2[^1LE_A] \tag{S3}$$

An analogous relationship can be deduced for the transient ^1ET_A state of species A:

$$\frac{d[^1ET_A]}{dt} = k_{2a}[^1LE_A] - k_3[^1ET_A] \tag{S4}$$

Finally, formation of the relaxed ground state depends only on the decay rate k_3 of the ^{1}ET state, giving

$$\frac{d[GS_A]}{dt} = k_3[^1ET_A]\ . \tag{S5}$$

Equation (S2) represents a first order process, which after integration yields (S6) describing the time dependent concentration of the initially formed FC_A state.

$$[\mathrm{FC_A}] = [\mathrm{FC_A}]_0 \exp(-k_1 t) \tag{S6}$$

Substituting this expression for FC in equation (S3), and solving the resulting differential equation gives

$$[^1\mathrm{LE_A}] = k_1[\mathrm{FC_A}]_0 \frac{\left(\exp(-k_{2a}t) - \exp(-k_1 t)\right)}{k_1 - k_{2a}} \tag{S7}$$

Similarly, the differential equation (S4) can be solved for ^1ET_A by substituting expression (S7) for ^1LE_A, yielding

$$[^1\mathrm{ET_A}] = k_1 k_{2a}[\mathrm{FC_A}]_0 \left(\frac{\exp(-k_1 t)}{(k_1 - k_{2a})(k_1 - k_3)} + \frac{\exp(-k_{2a} t)}{(k_1 - k_{2a})(k_3 - k_{2a})} - \frac{\exp(-k_3 t)}{(k_1 - k_3)(k_3 - k_{2a})} \right) \tag{S8}$$

Finally, formation of the ground state upon charge recombination can be expressed based on the time-dependent changes of ^1LE_A and ^1ET_A, giving

$$[\mathrm{GS_A}] = [\mathrm{FC_A}]_0 - [^1\mathrm{LE_A}] - [^1\mathrm{ET_A}] \tag{S9}$$

Next, species B is also assumed to undergo the ET reaction faster than radiative deactivation; however, the ET rate constant k_{2b} for species B is assumed to be smaller compared to k_{2a}. Vibrational cooling and charge recombination of species B are expected to be very similar compared to species A. Therefore, the same rate constants k_1 and k_3, respectively, were used to model these processes.

$$\mathrm{FC_B} \xrightarrow{k_1} {}^1\mathrm{LE_B} \xrightarrow{k_{2b}} {}^1\mathrm{ET_B} \xrightarrow{k_3} \mathrm{GS_B} \tag{S10}$$

Following the same procedure as outline above, the following equations describe the time-dependent evolution of each transient species originating from B:

$$[\mathrm{FC_B}] = [\mathrm{FC_B}]_0 \exp(-k_1 t) \tag{S11}$$

$$[^1\mathrm{LE_B}] = k_1[\mathrm{FC_B}]_0 \frac{\left(\exp(-k_{2b}t) - \exp(-k_1 t)\right)}{k_1 - k_{2b}} \tag{S12}$$

$$[^1\mathrm{ET_B}] = k_1 k_{2b}[\mathrm{FC_B}]_0 \left(\frac{\exp(-k_1 t)}{(k_1 - k_{2b})(k_1 - k_3)} + \frac{\exp(-k_{2b} t)}{(k_1 - k_{2b})(k_3 - k_{2b})} - \frac{\exp(-k_3 t)}{(k_1 - k_3)(k_3 - k_{2b})} \right) \tag{S13}$$

$$[\mathrm{GS_B}] = [\mathrm{FC_B}]_0 - [^1\mathrm{LE_B}] - [^1\mathrm{ET_B}] \tag{S14}$$

Finally, the third species C is assumed to undergo only radiative deactivation through a charge transfer state ^{1}CT, but not formation of the electron transfer state ^{1}ET.

$$FC_C \xrightarrow{k_1} {}^1LE_C \xrightarrow{k_{2c}} {}^1CT_C \xrightarrow{k_4} GS_C \quad \text{(S15)}$$

In analogy to above treatment, the time-dependent concentration changes of the transient species derived from component C were obtained:

$$[FC_C] = [FC_C]_0 \exp(-k_1 t) \quad \text{(S16)}$$

$$[{}^1LE_C] = k_1 [FC_C]_0 \frac{\left(\exp(-k_{2c} t) - \exp(-k_1 t)\right)}{k_1 - k_{2c}} \quad \text{(S17)}$$

$$[{}^1CT_C] = k_1 k_{2c} [FC_C]_0 \left(\frac{\exp(-k_1 t)}{(k_1 - k_{2c})(k_1 - k_4)} + \frac{\exp(-k_{2c} t)}{(k_1 - k_{2c})(k_4 - k_{2c})} - \frac{\exp(-k_4 t)}{(k_1 - k_4)(k_4 - k_{2c})} \right) \quad \text{(S18)}$$

$$[GS_C] = [FC_C]_0 - [{}^1LE_C] - [{}^1CT_C] \quad \text{(S19)}$$

The observed transient absorption at wavelength λ, $I(\lambda)$, can be now expressed as the sum of the fractional concentration of each transient species multiplied by the corresponding differential molar extinction coefficients. Since the chromophore is identical for all coordination species A, B, and C, the absorption coefficients of the respective transient species were approximated with a single set of constants $\Delta\varepsilon_{FC}$, $\Delta\varepsilon_{LE}$, $\Delta\varepsilon_{ET}$, and $\Delta\varepsilon_{CT}$. Thus, $I(\lambda)$ can be written as

$$I(\lambda) = \Delta\varepsilon_{FC}(\lambda) \cdot ([FC_A] + [FC_B] + [FC_C]) + \Delta\varepsilon_{LE}(\lambda) \cdot ([{}^1LE_A] + [{}^1LE_B] + [{}^1LE_C])$$

$$+ \Delta\varepsilon_{ET}(\lambda) \cdot ([{}^1ET_A] + [{}^1ET_B]) + \Delta\varepsilon_{CT}(\lambda) \cdot [{}^1CT_C] \quad \text{(S20)}$$

where $[FC_x]$, $[{}^1LE_x]$, $[{}^1ET_x]$, and $[{}^1CT_C]$ are the time-dependent concentrations of the respective transients as defined by equations S6-S8, S11-S13, and S16-S18. Note that the differential absorption extinction coefficient of the ground state species is by definition zero, and therefore, does not contribute to the absorption in equation (S20).

3. Molar-ratio Titration of Ligand 3 with $[Cu(I)(CH_3CN)_4]PF_6$ in CD_3OD

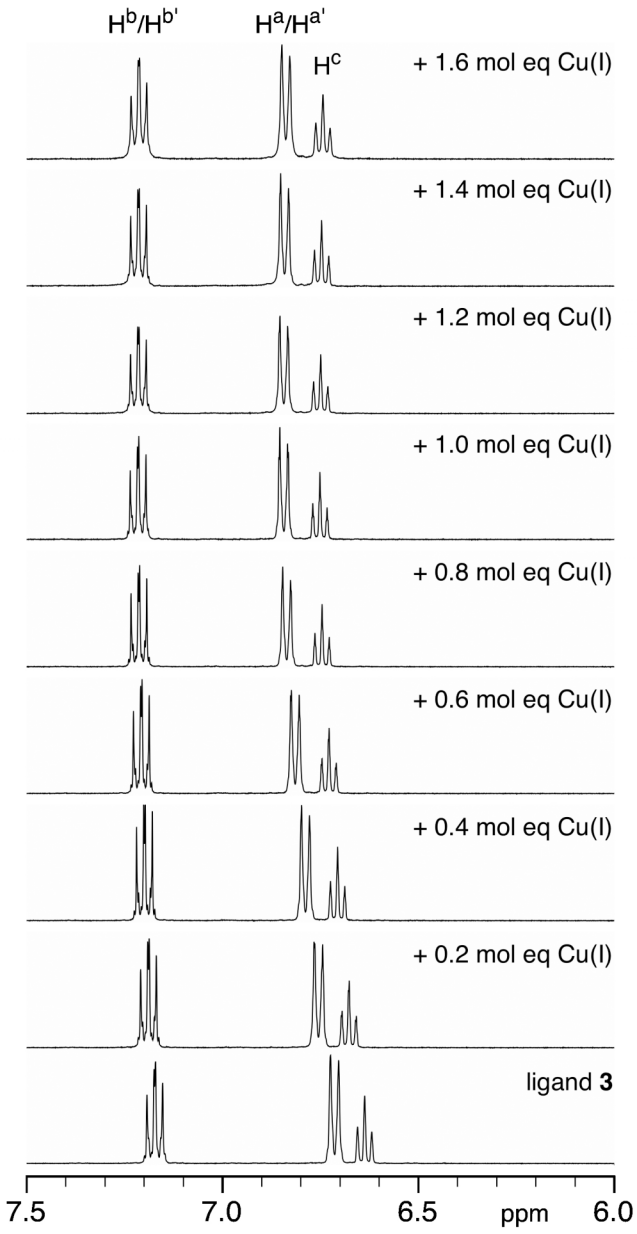

Figure S1: ^1H NMR spectra (aromatic region) for the titration of ligand **3** with $[Cu(I)(CH_3CN)_4]PF_6$ in CD_3OD at 298 K.

4. Electrochemical Data

Table S1: Donor and Acceptor Reduction Potentials and Electron Transfer Parameters of Pyrazoline Derivatives **1a-1e**.

	$E_{1/2}(D^+/D)^a$ (V)	$E_{1/2}(A/A^-)^a$ (V)	$\Delta E_{00}{}^b$ (eV)	$\Delta G_{et}{}^c$ (eV)
1a	0.47	–2.21	2.85	–0.22
1b	0.47	–2.19	2.92	–0.31
1c	0.49	–2.17	3.00	–0.39
1d	0.49	–2.22	3.13	–0.47
1e	0.50	–2.16	3.15	–0.54

[a] Half-wave potential in acetonitrile/0.1 M Bu_4NPF_6 vs. $Fc^{+/0}$ at 298K. [b] Zero-zero transition energy in methanol; estimated based on $\Delta E_{00} = (E_{abs}(max)+E_{em}(max))/2$. [c] Electron transfer free energy change calculated on the basis of the Rehm-Weller equation (1) with $w_p = -0.045$ eV.

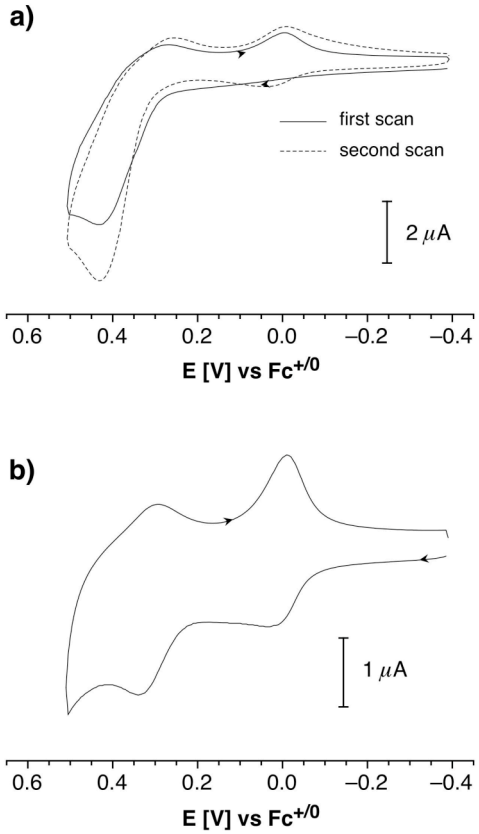

Figure S2: Cyclic voltammograms for (a) ligand **3** (100 μM) and (b) dimer **6** (50 μM) in methanol (0.1 M Bu_4NPF_6, glassy carbon working electrode, Pt counter electrode, aqueous Ag/AgCl/3M KCl reference electrode, scan rate 50 mV/s).

5. Oxidative Dimerization of Ligand 3 (UV-vis Spectra)

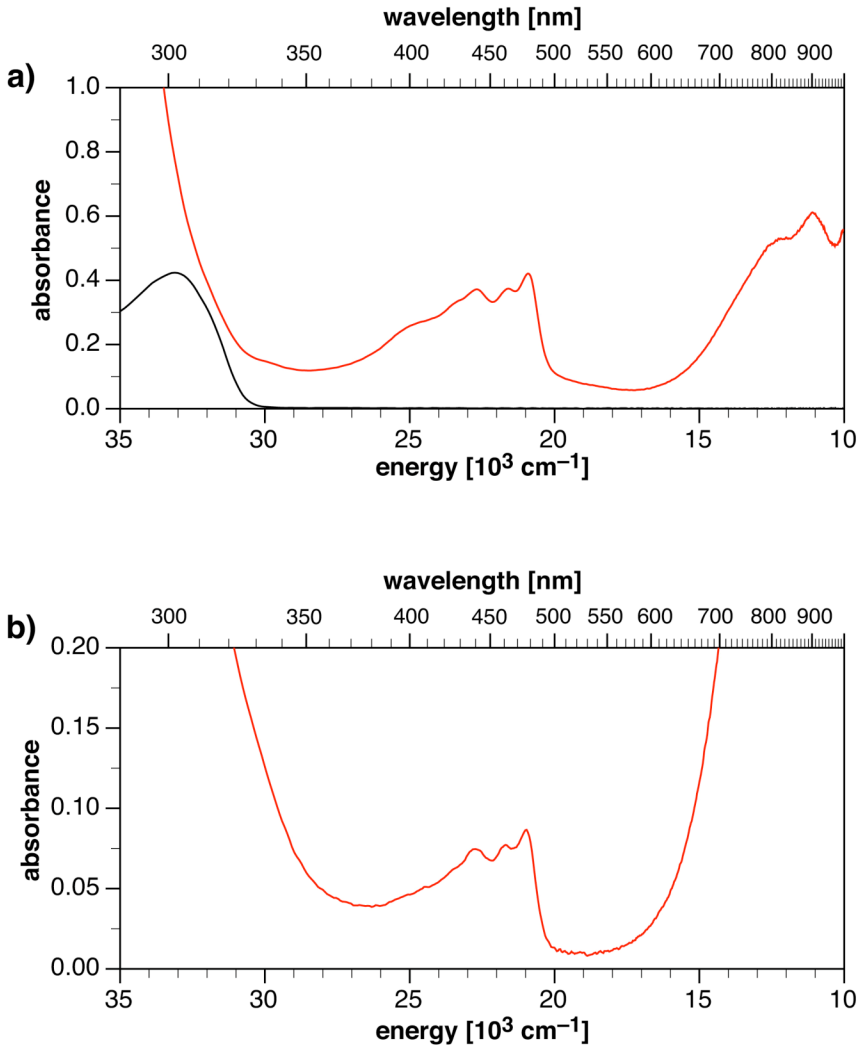

Figure S3: UV-vis spectra of (a) ligand **3** (50 µM) and (b) dimer **6** in methanol after treatment with 50 mM $Cu(OTf)_2$. For comparison, panel (a) also shows ligand **3** (50 µM) prior to addition of the Cu(II) salt (black trace).

6. Time-resolved Fluorescence Emission Decay Data

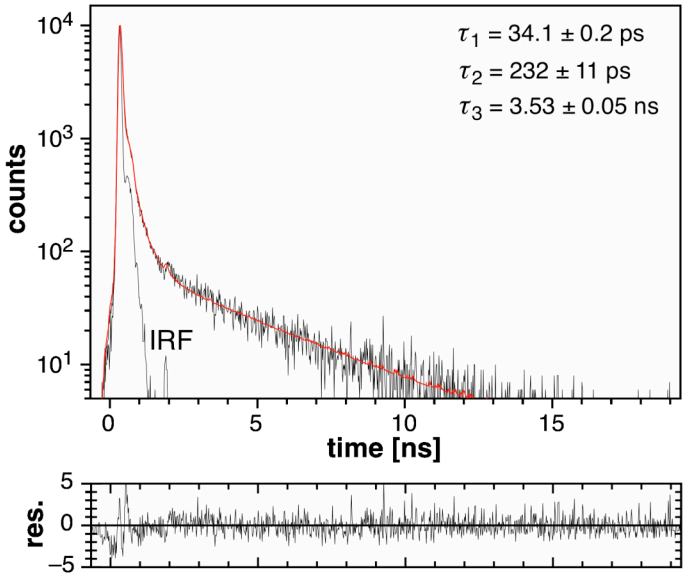

Figure S4a: Fluorescence decay profile for pyrazoline derivative **1a** in methanol at 298 K (IRF = instrument response function; red trace = fitted data).

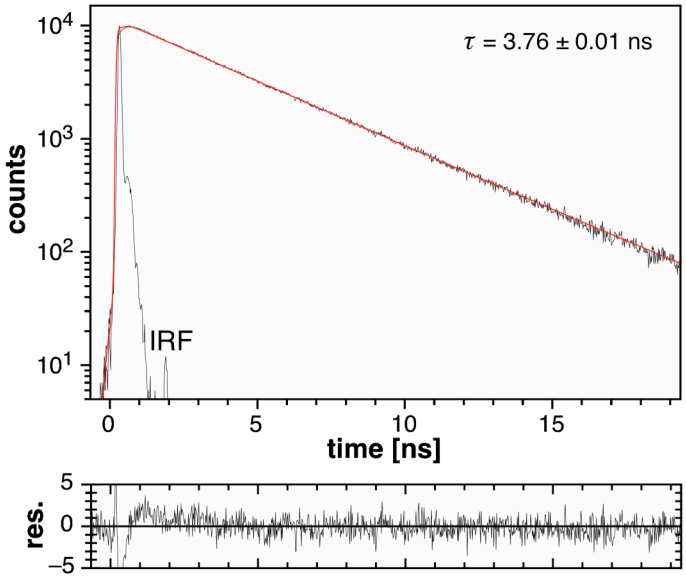

Figure S4b: Fluorescence decay profile for pyrazoline derivative **1a** in methanol containing 180 mM trifluoro acetic acid at 298 K (IRF = instrument response function; red trace = fitted data).

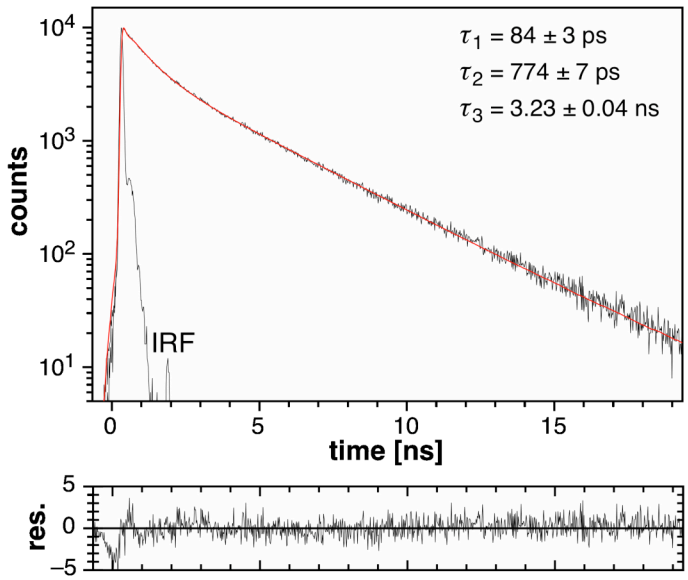

Figure S4c: Fluorescence decay profile for pyrazoline derivative **1a** in methanol/0.1% acetonitrile containing 10 µM $Cu(I)(CH_3CN)_4PF_6$ at 298 K (IRF = instrument response function; red trace = fitted data).

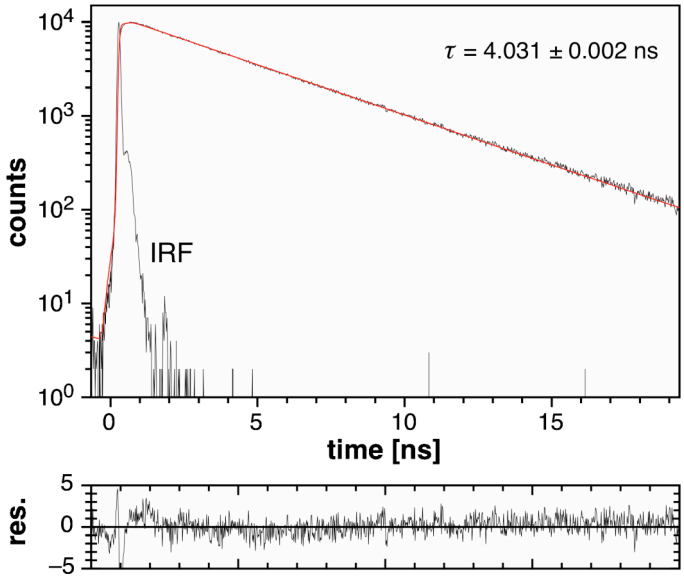

Figure S4d: Fluorescence decay profile for pyrazoline derivative **1a** in dichloromethane/0.1% acetonitrile containing 10 µM $Cu(I)(CH_3CN)_4PF_6$ at 298 K (IRF = instrument response function; red trace = fitted data).

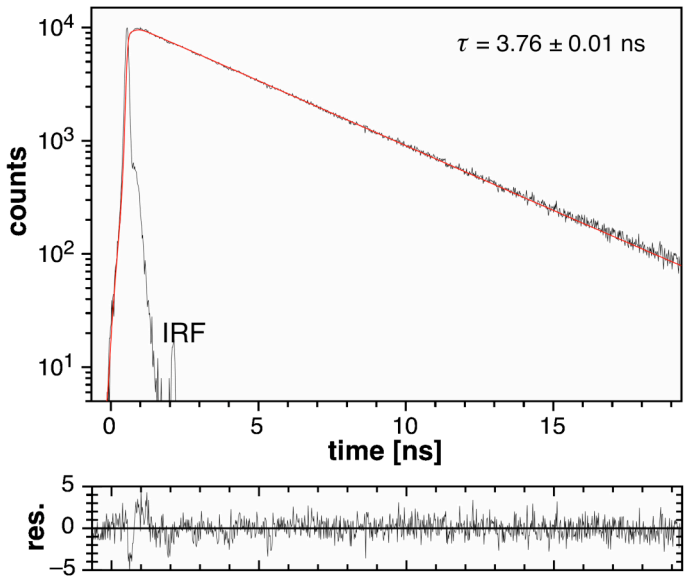

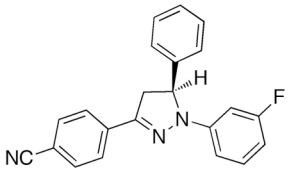

(±)-**2**

Figure S5: Fluorescence decay profile for pyrazoline derivative (±)-**2** in methanol at 298 K (IRF = instrument response function; red trace = fitted data).

7. Quantum Chemical Calculations

All geometry optimization and frequency calculations were performed at the B3LYP/6-31G(d) level of theory, an approach that has been previously used to successfully model the stability of monovalent copper complexes with neutral ligands in the gas phase.[S6] Single point energy calculations were performed at the B3LYP/6-31+G(d,p) level using the B3LYP/6-31G(d)-optimized geometries and corrected with prescaled zero point energies obtained from the frequency calculations. The geometry of the tetradentate complex [**3**-Cu(I)]$^+$ was optimized starting from the x-ray structure coordinates of the Cu(I) complex of the structurally related [16]aneN_2S_2 macrocycle 1,5-dithia-9,13-diazacyclohexadecane.[S7] To ensure that the N-aryl ring adopts the lowest energy conformation, the conformational space for rotation about the C(aryl)-N bond was systematically probed. The structures of all geometry-optimized complexes are depicted in Figure S6. A compilation of the relevant computational results is given in Tables S2 and S3.

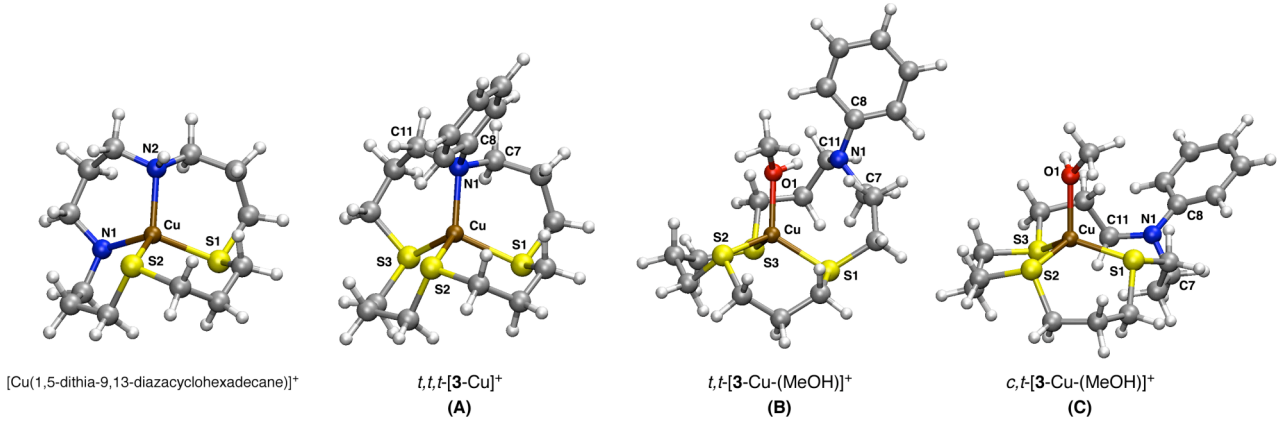

Figure S6: Computational structures and numbering schemes for Cu(I) complexes of ligand **3** with methanol as the auxiliary ligand. All geometries were optimized at the B3LYP/6-31G(d) level of theory. For comparison, the crystal structure geometry of the Cu(I) complex with 1,5-dithia-9,13-diazacyclohexadecane[S7] is shown to the left.

Table S2: Selected Structural Data for the Geometry Optimized Cu(I) Complexes of Ligand **3** with Methanol as an Auxiliary Ligand.[a]

Species	Cu-N (Å) [c]	Cu-S (Å) [d]	Σ [e]	Θ [f]
CCSD VEMWAL [b]	2.05-2.06	2.25-2.26	n/a	79.7
t,t,t-[**3**-Cu(I)]$^+$	2.06	2.26-2.30	326.7	82.5
t,t-[**3**-Cu(I)(MeOH)]$^+$	3.73	2.25-2.29	336.7	87.6
c,t-[**3**-Cu(I)(MeOH)]$^+$	4.62	2.23-2.26	351.0	83.3

[a] B3LYP/6-31G(d) level of theory. [b]Crystal structure of [1,5-dithia-9,13-diazacyclohexadecane-copper(I)]tetrafluoro-borate (Cambridge crystallographic database, code VEMWAL).[S7] [c]Range of Cu-N distances. [d]Range of Cu-S distances. [e]Sum of bond angles at N1 (C7-N1-C8, C8-N1-C11, C7-N1-C11). [f]Angle Θ between planes defined by S1-Cu-N1(O1) and S2-Cu-S3(N1) (atom numbering according to Figure S6).

Table S3: Computational Data for the Geometry Optimized Cu(I) Complexes of Ligand **3** with Methanol as an Auxiliary Ligand.[a]

Species	Electronic energy (Hartree)	ZPVE [b] (kcal/mol)	ΔH_{aux} [c] (kcal/mol)	HOMO energy (eV)	donor obital energy [d] (eV)
MeOH	-115.71426	32.2			
MeCN	-132.75419	28.6			
t,t,t-[**3**-Cu(I)]$^+$	-3592.84303	281.8	0	-8.239	-9.746
t,t-[**3**-Cu(I)(MeOH)]$^+$	-3708.56762	316.3	–12.4	-8.306	-9.001
c,t-[**3**-Cu(I)(MeOH)]$^+$	-3708.56475	315.5	–10.2	-7.824	-7.824

[a]B3LYP/6-31+G(d,p)//B3LYP/6-31G(d) level of theory. [b]Zero point vibrational energy. [c]Association enthalpy as defined by equation (5); calculated based on the differences in electronic energies at the B3LYP/6-31+G(d,p) level of theory and corrected with the corresponding scaled ZPVE's. [d]homologous to the aniline HOMO with B_2 symmetry.

Table S4-1: Cartesian Atomic Coordinates for the Geometry Optimized Structure of Methanol (B3LYP/6-31G(d)).

Atom	x/Å	y/Å	z/Å
O	0.749557	-0.122549	0.000000
H	1.131298	0.767379	0.000000
C	-0.662328	0.019146	0.000000
H	-1.036287	0.544398	-0.892945
H	-1.036287	0.544398	0.892945
H	-1.081214	-0.990659	0.000000

Table S4-2: Cartesian Atomic Coordinates for the Geometry Optimized Structure of Acetonitrile (B3LYP/6-31G(d)).

Atom	x/Å	y/Å	z/Å
H	1.026446	0.000000	1.560774
C	0.000000	0.000000	1.180897
H	-0.513223	-0.888928	1.560774
H	-0.513223	0.888928	1.560774
C	0.000000	0.000000	-0.280538
N	0.000000	0.000000	-1.440639

Table S4-3: Cartesian Atomic Coordinates for the Geometry Optimized Structure of Complex *t,t,t*-[**3**-Cu(I)]$^{+}$ (B3LYP/6-31G(d)).

Atom	x/Å	y/Å	z/Å
S	0.619831	-1.374153	2.011782
Cu	0.546721	0.127673	0.268533
S	1.180955	-1.191164	-1.500008
S	2.229293	1.624268	0.504631
N	-1.219964	1.177271	0.298319
C	-0.088193	-2.913557	1.299042
C	-0.695884	-0.784983	3.147112
C	3.717628	1.148292	-0.471379
C	1.517062	3.027296	-0.437641
C	3.018020	-1.178157	-1.435172
C	0.736469	-2.945932	-1.179401
C	-1.546788	1.269987	1.762544
C	-2.314487	0.571798	-0.490011
H	1.326364	-3.552154	-1.874941
H	-0.307116	-3.005004	-1.508730
C	0.869752	-3.501808	0.245910
H	-1.071213	-2.710978	0.859566
H	-0.216509	-3.621571	2.123345
H	1.905629	-3.424768	0.598809
H	0.657878	-4.576072	0.172872
H	-0.171759	-0.121335	3.843702
H	-1.051548	-1.642684	3.727442
C	-1.868037	-0.060817	2.478639
H	-2.585785	0.171409	3.276353
H	-2.391161	-0.743069	1.802799
C	-1.055824	2.582592	-0.250083
H	-2.390641	1.961577	1.895368
H	1.393055	2.748046	-1.489662
H	2.218490	3.865334	-0.379416
H	-1.966333	3.143296	0.007629
C	0.162309	3.417536	0.177722
H	0.249707	3.490896	1.269049
H	-0.060301	4.435906	-0.163901
H	3.371940	-1.860889	-2.213080
H	3.364795	-1.547466	-0.464234
C	3.544323	0.247252	-1.701871
H	4.541836	0.150669	-2.149904
H	2.923356	0.736355	-2.463140
H	4.214804	2.081383	-0.756866
H	4.366196	0.656858	0.261747
H	-0.687520	1.742046	2.246403
H	-1.042711	2.486307	-1.338451
C	-4.334560	-0.519619	-2.121758
C	-3.644553	0.545121	-0.054869
C	-2.014269	0.070000	-1.763636
C	-3.014087	-0.467806	-2.571638

Table S4-3: Continued

Atom	x/Å	y/Å	z/Å
C	-4.642735	-0.007294	-0.863913
H	-3.927717	0.942016	0.912909
H	-1.001324	0.125196	-2.145114
H	-2.756650	-0.845944	-3.557032
H	-5.666210	-0.026682	-0.501314
H	-5.112854	-0.944709	-2.747968

Table S4-4: Cartesian Atomic Coordinates for the Geometry Optimized Structure of Complex *t,t*-[**3**-Cu(I)(MeOH)]$^{+}$ (B3LYP/6-31G(d)).

Atom	x/Å	y/Å	z/Å
S	-1.215813	-1.823967	-1.231484
Cu	-1.236950	-0.045507	0.146947
S	-3.015943	-0.171759	1.482006
S	-1.403869	1.810149	-1.182849
N	2.383066	0.356010	-0.670535
C	-2.378516	-3.026562	-0.456113
C	0.361375	-2.804193	-1.298480
C	-2.694043	2.934707	-0.477599
C	0.167146	2.762789	-0.986470
C	-4.103861	1.172838	0.835467
C	-3.972012	-1.709515	1.133284
C	1.888182	-0.739657	-1.536267
C	3.627765	0.076169	0.036029
H	-5.028720	-1.463988	1.281231
H	-3.687323	-2.390703	1.942606
C	-3.767755	-2.399550	-0.223254
H	-1.948523	-3.377201	0.488191
H	-2.461892	-3.876209	-1.139171
H	-4.024939	-1.727229	-1.051041
H	-4.501799	-3.215036	-0.263165
H	0.509340	-3.096560	-2.342724
H	0.206030	-3.719006	-0.718109
C	1.574147	-2.037136	-0.758642
H	2.434760	-2.713369	-0.786290
H	1.408955	-1.802865	0.296764
C	2.512314	1.645506	-1.417087
H	2.583981	-0.943481	-2.365335
H	0.516648	2.680743	0.045800
H	-0.083102	3.808035	-1.184678
H	3.225787	1.508496	-2.245369
C	1.230944	2.264989	-1.997923
H	0.772560	1.601274	-2.738914
H	1.573669	3.129099	-2.578984
H	-4.977991	1.219189	1.490640
H	-4.442121	0.918056	-0.174536
C	-3.344026	2.518338	0.847507
H	-4.069648	3.304271	1.092109
H	-2.605853	2.529930	1.659305
H	-2.233371	3.922074	-0.371199
H	-3.457648	3.016769	-1.257955
H	0.971011	-0.369344	-2.001419
H	2.970304	2.358425	-0.727277
C	6.005954	-0.329878	1.477266
C	4.572637	-0.855914	-0.406927
C	3.891696	0.809319	1.202679
C	5.073069	0.613277	1.914058
C	5.750700	-1.059516	0.317976

Table S4-4: Continued

Atom	x/Å	y/Å	z/Å
H	4.411487	-1.421770	-1.318210
H	3.169695	1.546546	1.545811
H	5.260039	1.191938	2.814062
H	6.473878	-1.789152	-0.034982
H	6.924469	-0.490063	2.033571
O	0.415613	0.427276	1.257153
C	0.707017	-0.110805	2.554020
H	1.223069	0.423400	0.655937
H	-0.182036	0.029771	3.172014
H	1.548765	0.417517	3.011579
H	0.939314	-1.182161	2.504882

Table S4-5: Cartesian Atomic Coordinates for the Geometry Optimized Structure of Complex *c,t*-[**3**-Cu(I)(MeOH)]$^{+}$ (B3LYP/6-31G(d)).

Atom	x/Å	y/Å	z/Å
S	-0.817138	-2.104188	0.350494
Cu	-1.519630	0.022247	0.623140
S	-3.767840	-0.173882	0.455857
S	-0.985233	1.730954	-0.707396
N	2.822302	-0.020337	-0.966183
C	-1.867545	-2.833689	-0.974779
C	0.878181	-2.257076	-0.349079
C	-2.411386	2.889626	-0.652764
C	0.421073	2.830556	-0.226376
C	-4.502340	1.387240	-0.186747
C	-4.017904	-1.334503	-0.954083
C	2.515999	-1.091004	-1.923464
H	-3.620907	-0.884950	-1.870157
H	-5.099162	-1.455476	-1.071279
C	-3.373865	-2.708102	-0.694592
H	-1.599661	-3.892627	-1.040111
H	-1.619515	-2.361896	-1.931334
H	-3.871891	-3.416409	-1.368138
H	-3.605791	-3.048469	0.322284
H	1.157596	-3.314871	-0.307581
H	1.489856	-1.715406	0.379706
C	1.092685	-1.658133	-1.744042
H	0.362690	-0.859417	-1.919559
H	0.916909	-2.411518	-2.520620
C	2.177035	1.253924	-1.272602
H	3.251885	-1.888464	-1.802506
H	0.148000	3.369607	0.686831
H	0.547096	3.564613	-1.029869
H	1.305410	1.020467	-1.888926
C	1.695791	2.006314	-0.010033
H	2.472851	2.682840	0.361972
H	1.524638	1.267319	0.782122
H	-4.710203	1.971379	0.716729
H	-5.470688	1.118932	-0.621803
C	-3.694100	2.226928	-1.187521
H	-3.459103	1.647179	-2.088545
H	-4.362590	3.033832	-1.514413
H	-2.556073	3.252624	0.371035
H	-2.147960	3.741678	-1.286155
H	2.622684	-0.731208	-2.959942
H	2.810594	1.911668	-1.889944
C	4.108636	-0.005282	-0.360588
C	6.633077	-0.023765	0.918587
C	4.623057	-1.181849	0.219025
C	4.885164	1.162176	-0.275525
C	6.128003	1.148549	0.361665

Table S4-5: Continued

Atom	x/Å	y/Å	z/Å
C	5.868752	-1.190429	0.838730
H	4.037940	-2.096574	0.197929
H	4.538018	2.088845	-0.718719
H	6.706498	2.067280	0.407970
H	6.238245	-2.115240	1.273569
H	7.601135	-0.030930	1.409637
O	-1.042073	0.509152	2.615876
H	-0.422771	1.235982	2.777255
C	-1.139471	-0.296477	3.811027
H	-1.460428	0.315852	4.659131
H	-0.183790	-0.781306	4.035234
H	-1.893461	-1.057557	3.609097

8. References:

(S1) Burdon, J.; Hollyhead, W. B. *J. Chem. Soc.* **1965**, 6326.
(S2) Cody, J.; Mandal, S.; Yang, L.; Fahrni, C. J. *J. Am. Chem. Soc.* **2008**, *130*, 13023.
(S3) Everett, J. L.; Ross, W. C. J. *J. Chem. Soc.* **1949**, 1972.
(S4) Goodrow, M. H.; Musker, W. K. *Synthesis* **1981**, 457.
(S5) Binstead, R. A.; Zuberbühler, A. D.; 3.0.27 ed.; Spectrum Software Associates, Marlborough MA 01752: 2001.
(S6) Luna, A.; Amekraz, B.; Tortajada, J. *Chem. Phys. Lett.* **1997**, *266*, 31; Rannulu, N. S.; Rodgers, M. T. *Phys. Chem. Chem. Phys.* **2005**, *7*, 1014; Yang, Z.; Rannulu, N. S.; Chu, Y.; Rodgers, M. T. *J. Phys. Chem. A* **2008**, *112*, 388.
(S7) Balakrishnan, K. P.; Riesen, A.; Zuberbühler, A. D.; Kaden, T. A. *Acta Crystallogr. C* **1990**, *46*, 1236.

Complete Reference (20):

Shao, Y.; Molnar, L. F.; Jung, Y.; Kussmann, J.; Ochsenfeld, C.; Brown, S. T.; Gilbert, A. T. B.; Slipchenko, L. V.; Levchenko, S. V.; O'Neill, D. P.; DiStasio, R. A.; Lochan, R. C.; Wang, T.; Beran, G. J. O.; Besley, N. A.; Herbert, J. M.; Lin, C. Y.; Van Voorhis, T.; Chien, S. H.; Sodt, A.; Steele, R. P.; Rassolov, V. A.; Maslen, P. E.; Korambath, P. P.; Adamson, R. D.; Austin, B.; Baker, J.; Byrd, E. F. C.; Dachsel, H.; Doerksen, R. J.; Dreuw, A.; Dunietz, B. D.; Dutoi, A. D.; Furlani, T. R.; Gwaltney, S. R.; Heyden, A.; Hirata, S.; Hsu, C. P.; Kedziora, G.; Khalliulin, R. Z.; Klunzinger, P.; Lee, A. M.; Lee, M. S.; Liang, W.; Lotan, I.; Nair, N.; Peters, B.; Proynov, E. I.; Pieniazek, P. A.; Rhee, Y. M.; Ritchie, J.; Rosta, E.; Sherrill, C. D.; Simmonett, A. C.; Subotnik, J. E.; Woodcock, H. L.; Zhang, W.; Bell, A. T.; Chakraborty, A. K.; Chipman, D. M.; Keil, F. J.; Warshel, A.; Hehre, W. J.; Schaefer, H. F.; Kong, J.; Krylov, A. I.; Gill, P. M. W.; Head-Gordon, M. *Phys. Chem. Chem. Phys.* **2006**, *8*, 3172-3191.